STEMedicine

REVIEW ARTICLE

Plasmonic nanoassemblies for surface-enhanced Raman scattering-based biodetection and biomedical theranostics

Yi Chen[1,2*], Yu Bai[1,2†], Heng Zhang[1,2†] and Zheng Zhou[1,2]

[1]State Key Laboratory of Bioelectronics, Jiangsu Key Laboratory for Biomaterials and Devices, School of Biological Science and Medical Engineering, Southeast University, Nanjing, China; [2]Southeast University-Monash University Joint Research Institute, Suzhou, China

Abstract

Plasmonic nanoassemblies are well-defined organizing of elementary metallic nanocrystal building blocks into ordered architectures across multiple scales, which constituents an exciting route to engineer nanomaterials structures with novel properties. Such nanoassemblies can accurately enhance, guide, and switch electromagnetic field at the nanoscale, which is shaping new-generation technologies with a plethora of applications, such as ultrasensitive bimolecular sensors, cancer diagnostics, and photothermal therapy (PTT), to name a few. In this review, we mainly focus on the plasmonic nanoassemblies, including the structure design, property control, and biomedical applications. The guiding principles have been first clarified with design rules being suggested. Then, the methodologies for fabrication of surface-enhanced Raman scattering-based (SERS-based) biodetection devices have been discussed. Finally, we summarized the PTT by using the plasmonic nanoassemblies as bioprobes for theranostics. Based on the facile yet efficient fabrication methods, high-efficient optoelectronic properties, and high performance in biomedical applications, we firmly believe that the plasmonic nanoassemblies can be integrated with portable devices for next-generation biosensors and biomedical theranostics.

Keywords: *plasmonic*; *nanoassemblies*; *surface-enhanced Raman scattering*; *biodetection*; *theranostics*

Received: 4 September 2022; Revised: 7 September 2022; Accepted: 8 September 2022; Published: 10 October 2022

The rapid advances and substantial progress in the controllable synthesis of plasmonic nanoparticles with noble metallic compositions have provided versatile building blocks for the nanoengineering of nanoassemblies. Due to the unique optical properties, facile surface chemistry, and appropriate size scale of the plasmonic nanocrystals, much enthusiasm and great efforts have been generated in assembling such elementary building blocks into well-defined assemblies, such as plasmonic dimer/multimers (1, 2), linear structures (3, 4), 2D superlattice sheets, and 3D supracrystals (5–10). By integrating bottom-up assembly method with top-down lithography, multidimensional nanoassemblies have been fabricated at the nanoscale with sufficient degree of control over the material size, shape, composition, and morphology. It is expected that the ability to manipulate these elementary nanoparticles into well-defined assemblies will further impact the way materials are synthesized and devices are fabricated. The fabrication of such plasmonic nanoassemblies has led to a wide spectrum of applications, including miniaturized optical (11) and electronic devices (12, 13), biosensors (14, 15), and biomedical diagnostics and therapeutics (16, 17) (Fig. 1).

The plasmonic nanoassemblies constitute an exciting route not only to engineer material structures at nanoscopic dimensions with high accuracy but also to create novel properties different from their bulk counterparts at multiple length scales to integrate multifunctionalities into well-defined multi-material composites. Under the guiding of basic theoretical laws and predictions (18), the plasmonic coupling and hybridization effects can be designed with well-defined methodology. Among those functions, surface-enhanced Raman scattering (SERS) represents a rapidly developed, expanding method for ultrasensitive

[†]These authors contributed equally to this work.

detection of biomolecules, such as cancer biomarkers and specific protein. Also, the SERS devices that being assembled by plasmonic nanocrystals can be applied in real-time detection of trace chemicals for *in situ* chemical reaction monitoring; metal-catalyzed reactions monitoring; molecular imaging; evaluating microorganisms, cells, and tissues; and even *in vivo*. However, there is still a great challenge to fabricate efficient and reproducible SERS substrates due to the complex forces and interactions among nanoparticles. Apart from the plasmonic imaging and sensing for diagnostics, the ability of plasmonic nanoassemblies to convert strongly absorbed light efficiently into localized heat can be exploited for the selective photothermal therapy (PTT) of cancer and bacterial infection, which paves promising avenue for biomedical theranostics and precise medicine for health monitoring.

Here, in this review, we begin with the introduction of basic theoretical principles for controlling the plasmonic properties of individual nanocrystals and nanoassemblies. Based on the optoelectronic laws and electromagnetic enhancement of nanoparticles, we then summarize the representative methods for the construction of SERS substrates from the point of view of materials design. The recent advances in SERS-based plasmonic nanostructures for biodetection have been described, including the enhancement of SERS activity and high sensitivity with different shapes and morphologies, and briefly expounded the bio-diagnostic applications based on SERS. Finally, we summarized the typical therapeutic strategies by using the plasmonic nanoassemblies and mainly focus on the progresses in PTT for biomedical theranostics.

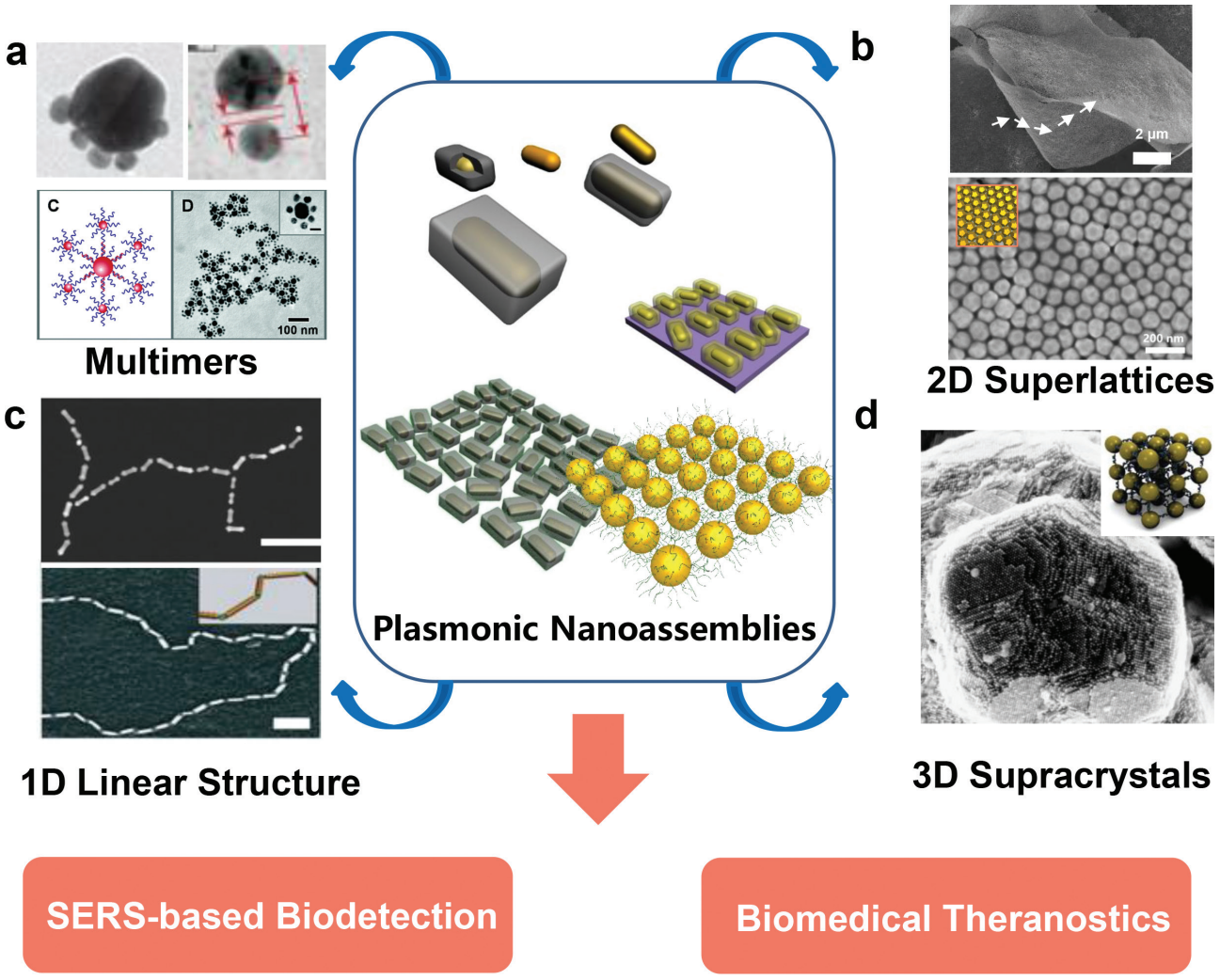

Fig. 1. Plasmonic nanoassemblies with multidimensional structures assembled from libraries of plasmonic atoms. (a) Plasmonic multimers (19–21). (b) 2D superlattice sheets (22, 23). (c) Linear and branch 'polymeric chain' assembled by Au nanorods (3, 4). (d) 3D Au nanoparticles (AuNPs) supracrystals controlled by DNA (10).

Basic plasmonic theories and design rules for the nanoassemblies

The fundamental property of plasmonic nanoassemblies is the localized surface plasmon resonance (LSPR), which is induced by the coherent collective oscillations of conduction electrons upon interaction with electromagnetic radiation (24). According to the classical Mie theory (25), the optical properties are strongly affected by structural parameters, such as morphology, material composition, the surrounding dielectric property, and interparticle interactions (26, 27). The extinction cross-section, C_{ext}, for the scattering of a metallic nanosphere is given by (28):

$$C_{ext}(\omega, R) = 12\pi \frac{\omega R^3 \varepsilon_m^{3/2}}{C} \frac{\varepsilon_2(\omega, R)}{[\varepsilon_1(\omega, R) + 2\varepsilon_m]^2 + \varepsilon_1(\omega, R)^2} \quad (1)$$

where R is the radius of nanosphere, c is the speed of light, ε_m is the dielectric constant of the surrounding medium (assumed to be frequency independent), ω is the frequency, and $\varepsilon(\omega, R) = \varepsilon_1(\omega, R) + i\varepsilon_2(\omega, R)$, in which $\varepsilon_1(\omega, R)$ and $i\varepsilon_2(\omega, R)$ are the real and complex parts of the material dielectric constant, respectively. Based on this principle, controlling the size and morphology of nanocrystals is the one feasible way to engineer the wavelength and distinction strength of LSPR bands (29).

Accordingly, it is important to develop high-efficient chemical synthesis method for controlling the particle sizes and shapes. Moreover, rational design of nanoparticle-assembled nanostructures is in urgent need for unravelling the multifunctionality (28). By programming the resonance frequencies and coupling effects of plasmonic nanoparticles under the guidance of other theoretical predictions, such as plasmon hybridization theory, well-defined architectures and novel optoelectronic properties may be generated for real-world biomedical applications.

SERS-based nanoassemblies for the detection of biomarkers

Electromagnetic field is generated between any plasmonic nanoparticles near each other. It is the local enhancement of these electromagnetic fields that causes high signal of SERS. When plasmonic nanoparticles are closed enough even to a few nanometers, LSPR will be obtained and coupled, resulting in enhanced electromagnetic fields (30) called hotspots. It is generally believed that the main methods to increase the SERS activity to obtain higher SERS signals are to form as many hot spots as possible, and they can be generally divided into three types.

The first is that under the induction of various microscopic forces, the noble metal nanoparticles may self-assemble on the substrate as close as possible to form hot spots; the second way is to control the specific shape of the substrate, and novel metal nanoparticles will be placed close to each other when they are deposited on them by using the top-down template method. The third is to prepare plasmonic nanoparticles with very sharp tips or irregular morphology such as core-shell satellite and multi-branched nanoparticles.

Accordingly, great efforts were put into improving the sensitivity *via* evaluating different noble metal shapes from simply structures to complex structures. In addition to synthesizing advanced nanostructures, the development of effective Raman-labeled compounds that can resonate with excitation light also attracted much interest. By appropriate integration and hybridization, plasmonic nanoparticles combining of noble metal and other materials like metallic oxide, non-metallic oxide, and magnetic nanoparticle were synthesized.

The use of bimetallic systems for substrate preparation is an effective way to optimize SERS detection. Novel metal alloy nanoparticles, particularly Au-Ag alloys and Au-Cu alloys, can generate strong LSPR coupling under visible radiation excitation, which were acting as excellent candidates for SERS substrates. The SERS effect can be controlled by changing the bimetallic system composition to adjust the LSPR coupling (31). For example, the incorporation of a small amount of Au in Ag nanoparticles can effectively improve the SERS effect. Rao et al. (31) synthesized Ag-Au bimetallic nanoparticles for the preparation of a stable and uniform SERS substrate using a two-step method, and the substrate showed about 10^8 enhancement factors (EFs) and a detection limit of 0.6 pmol for the detection of rhodamine 6G. The research of M. Bańkowska group[2] mainly focuses on the Au-Cu bimetallic nanostructures. The substrate is prepared by sputter deposition of the Au-Cu bimetallic thin film layer on nanostructured GaN prepared by photolithography. The preparation process was etching hexagonal etch pits with six inverted pyramids on the surface of nanostructured GaN, and sputter Au-Cu alloys on the surface to form an SERS measurement platform. It is reported that gold is not as effective as silver, but the silver surface is easily oxidized and not biocompatible. However, Au-Cu alloy nanoparticles have been reported that can be used for catalysis, so the use of Au and Cu alloys as SERS measurement platforms was explored by them. The experiment not only compares the influence of the percentage of Cu in the alloy Au-Cu layer on the SERS enhancement effect but also compares the difference in measurement effect of pyridine and 4-mercaptobenzoic acid when Au-Cu alloy and Au and Au-Ag alloy covered on the same GaN platform. Final experiments show that a moderate reduction of the percentage of Cu can increase the chemical stability of the substrate. The coated Au-Cu alloy is about one order of magnitude lower than that of the Au-Ag alloy, but the etch pit surface is an order of magnitude higher than that without the etch pit surface. Therefore, the etching sputtering method can also be used as simple and reproducible

method to manufacture sensitive SERS platforms with different plasma metal coatings.

Commonly used complex structures such as core-shell satellites and multi-branched structures and nanorosette particles can form enhanced electromagnetic fields for SERS signal enhancement. Core-shell nanostructures are one of the most common structures to improve SERS activity because they not only can enhance the LSPR but also increase the intensity of E-field. Common core-shell structures such as Au-Ag core-shell nanoshuttles (NS), core-shell satellite structures of Au and magnetic oxides, or non-metal oxides have been studied. Bai et al. (32) prepared core-shell Au-Ag nanoshuttles structures with Au nanorods as cores and Ag nanoparticles as shells with sharp tips at both ends and adjustable shell thickness. The morphology control was mainly achieved by adjusting the temperature of the reaction system containing the basic glycine buffer (pH8.5). This sharp-pointed Au-Ag NS has significantly improved refractive index sensitivity and SERS activity relative to the original Au NR and other Au nanostructures, which make these materials to have great potential in biomedical applications such as ultrasensitive sensing of biomarkers.

The combination of SERS performance with catalytic property by using multi-branched nanoparticles has also received extensive attention in recent years. Anisotropic nanostructures with rough surfaces can significantly improve SERS activity. On the surface of the transition metal Pd or Pt, or when the diameter of the metal particles is less than 10 nm, catalytic reaction can be observed. Au protrusions growing on the surface of the particles can produce some 'hot spots' to enhance the SERS effect, and the increased surface area of the protrusions and the number of low coordination atoms can also increase the catalytic activity. Cui et al. (33) fabricated Au@Pt nanoparticles with multi-branched structures by precisely controlling the amount of Pt sputter deposited on the Au@Pt surface. In the characterization, these particles show good SERS characteristics and extremely high catalytic activity, and these two characteristics can be regulated by adjusting the ratio of Pt and Au two metals.

Shin et al. (34) pointed out a simple way to prepare uniform Au nanorosette as a good SERS substrate for the detection of methylene blue (MB) and crystal violet (CV) with efficient EFs of 2.6×10^8 and 8.8×10^5, respectively. The assembly was conducted *via* the reduction of the $AuCl_4^-$ precursor by 2-thiopheneacetic acid (2-TAA), which was both as a reducing agent and a surface-stabilizing agent. The structures of Au nanoparticles strongly depend on the molar ratio of 2-TAA to $AuCl_4^-$. Under the high ratio state, the aggregate of nanorods and nanoparticles will be observed, in which Au nanorosette will be synthesized at low ratio.

Bifunctional nanoparticles integrate two formerly distinct functionalities into a single entity, which can provide superior and sometimes unprecedented properties (35). Multifunctional magnetic core-satellite nanostructure Fe_3O_4@SiO_2-Au substrate was synthesized *via* grafting Au NPs onto microsized Fe_3O_4 (36) for the charge selective detection of food dye molecules like sunset yellow, where the Fe_3O_4@SiO_2 is the core and the Au is the satellite. The charge of food dyes could be captured selectively *via* adjusting the gaps of Au nanoparticles and analyzed by SERS with high sensitivity due to the plenty of hotspots produced between core-shell-satellite 3D magnetic microspheres and assembled Au satellites. Meanwhile, three-dimensional finite difference time domain (FDTD) simulation, molecular dynamics (MD) simulations, and density function theory (DFT) calculations were conducted to research the most suitable Au nanoparticle gap and support the theory and result. Sinha et al. (37) investigated low-cost efficient and recyclable SERS-active substrates by sputter depositing Au nanoparticles onto ZnO nanorods for the detection of methylene blue. Apart from low fluorescence and excellent resistance against oxidation of Au, strong light confinement resulted by high refractive index contributes to increase the SERS effect vastly. In addition, taking advantages of the photocatalytic properties of ZnO to degrade the analyses under the UV light inducement, the substrates can be cleaned and reused.

Nanostructures that being assembled by Au and some non-metallic oxides show unique potential to be used as SERS tags for bioimaging applications. Rodríguez-Fernández et al. synthesized hybrid core-satellite colloidal particles that can closely contain different sized Au sphere particles, two different dye molecules then were loaded into these particle clusters for SERS imaging applications *in vivo*, and silica was covered outside them as a nano-antenna, which played the role of fixing and protecting nanostructures at the same time. In this study, the final geometry region can be produced successfully by controlling Au-SiO_2 particles to limit the assembly area. Zhong et al. (38) pointed out a new way to prepare SERS substrate through Poly(methyl methacrylate) (PMMA) template on insoluble liquid–liquid interface. Due to its excellent optical transparency, PMMA can be used as an ideal template for fixing self-assembled AuNPs. The insolubility of water and toluene will cause the AuNPs aqueous solution and PMMA toluene to separate, and adding ethanol to the aqueous solution of the AuNPs in the layered solution will change the density, so that the AuNPs will rise to the interface and self-assemble into an ordered layer with numerous 'hot spots'. At the same time, with the slow evaporation of the toluene solution, the PMMA molecules form a thin PMMA template constraining the assembly of the gold nanoparticle layer on the water/toluene interface.

Finally, using the polyethylene (PE) film as carrier to solve the AuNPs/PMMA film is too thin to remove the problem. The SERS substrate prepared by this method exhibits excellent reproducibility, high EF, and great potential both in the detection of the model molecule malachite green isothiocyanate and the detection of residual malachite green on the surface of irregular fish. Bekana et al. (39) claimed that in the existing methods for the preparation of SERS substrates using Au nanoparticle assembly, either preparing AuNPs first and then adding external inducer to induce assembly, or taking advantages of the template method to assemble the nanoparticles into an ordered structure, an external reagent/polymer linker both may interfere with SERS detection of trace analyses, and thus affect the SERS performance (Fig. 2a). Hence, they developed a novel method to prepare large-area, high-sensitivity and low-cost, high-efficiency SERS substrates using the polycrystalline ice (PCI) freezing method. In this method, the substrates are fabricated only count on the PCI microstructure without any external template or crosslinking agents. At cryogenic temperatures below –20°C, colloidal gold nanoparticles have very low solubility in ice crystals, so they can only be concentrated and packed together between growing ice crystals. Therefore, PCI can assemble colloidal nanostructures into a one-dimensional (1D) chain. The practicality of preparing SERS substrates in this way has been demonstrated by testing trace Thiram eluted from the apple fruit surface. In addition, researches about adjusting the size of AuNPs and AuNPs superstructure to optimize SERS activity are further explored.

Based on the efficient fabrication methods for the plasmonic nanoassemblies, the enhanced electromagnetic field can induce ultrahigh Raman signal for biomedical diagnostics. Cereal toxins such as ochratoxin A (OTA) and aflatoxin B1 (AFB1) are frequently found in cereal samples, which are toxic secondary metabolites released by fungi, and are generally carcinogenic, mutagenic, and hepatotoxic (40). The existing detection methods for them are generally immunoassay or fluorescence analysis, require expensive cost and tedious procedures, or are easily interfered by foreign substances such as oxygen and humidity. Zhao et al. (40) proposed that the SERS tags of core-shell satellite structures can enable more rapid and high-throughput detection of mycotoxins. The insertion of AFB1 (50 bp) and OTA (36 bp) Raman markers into the nucleus and shell junctions will avoid these mycotoxins from creating larger gaps between the nanoparticles, thereby reducing SERS signal problems, while at the same time passing through nuclear-shell satellites. The structure generates a large number of hotspots to amplify the SERS signal, enabling ultra-sensitive dual detection of OTA and AFB1 in corn flour.

The identification of cancerous B cells in lymphoma and leukemia is critical for early diagnosis and precise treatment. The diagnostic technique currently used is the fluorescence label detected by flow cytometry. The limitation of this technology is that only a single excitation source can be used, and the number of markers present on the cell surface that can be detected by a single excitation source is limited. However, narrow SERS bandwidths of 1 to 2 nm can solve this bandwidth issue (41). MacLaughlin et al. (41) proposed a SERS probe that fabricated by Au nanoparticles and can produce antibodies that target three surface-specific markers of malignant B cells from LY10 lymphoma cell lines (Fig. 2b). The SERS probe has good scattering near infrared wavelengths, and the wavelength is not strongly absorbed, thus reducing the possibility of sample damage or autofluorescence interference. In this experiment, they characterized the feasibility of SERS probes by a variety of methods. The use of SERS and confocal Raman imaging from cell suspensions confirmed the specificity of primary chronic lymphocytic leukemia and LY10 cells for granulosa cell markers, respectively. Fluorescence flow cytometry was used to confirm the binding of the SERS probe to LY10 on a large cell population.

The intense surface-plasmon-enhanced scattering from AuNPs makes them promising as optical probes and labels for imaging-based detection of cancers. One such technique for molecular specific labeling of cancer cells is the immunotargeting of nanoparticles by conjugating them with antibodies to antigens overexpressed on the diseased cells (42). Sokolov et al. employed immunotargeted AuNPs for the imaging of cervical epithelial cancer cells (SiHa cells) (43). Colloidal AuNPs 12 nm in diameter were conjugated to anti-EGFR (epidermal growth factor receptor) monoclonal antibodies via non-covalent electrostatic adsorption of the antibody molecules to the citrate-capped, negatively charged Au nanoparticle surface. The cell suspensions were labeled with the Au nanoparticle-antibody conjugates by simple incubation. Using a scanning confocal reflectance microscope, with a 647 nm laser to excite the nanoparticle SPR, SPR scattering of the Au nanoparticles labeling the cells was clearly demonstrated on an otherwise dark background.

Plasmonic nanoassemblies for PTT

PTT is demonstrated to be a satisfactory and comparatively innocuous alternative strategy to treat cancer, due to the high-efficiency for the heat transfer based on the photothermal effects of nanocrystals. By exposing bio-tissues to a relatively high temperature, it would destroy abnormal cells further effectively and promptly; therefore, the pain of the patients could be significantly relieved. Moreover, PTT causes little wound and no need for giant equipment, clinically appropriated for unresectable and hardly operable tumors therapy. PTT strategy approximately contains two procedures: photothermal conversion and specific-targeting treatment. The former is a

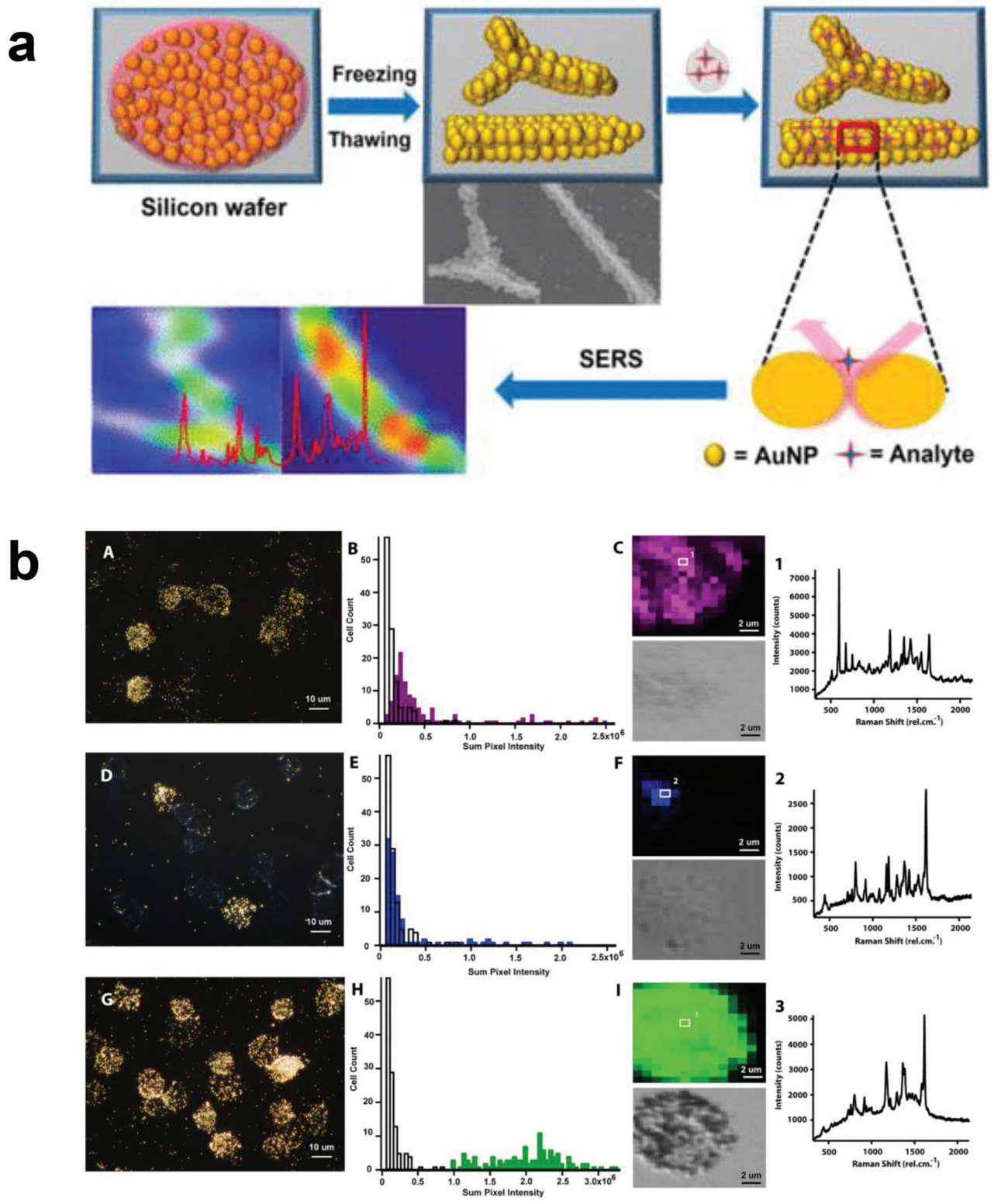

Fig. 2. (a) Plasmonic surface-enhanced Raman scattering (SERS) substrate made by using polycrystalline ice for assembly (39). (b) SERS-based imaging and analyzing of the LY10 B cell line (41).

pure physical energy transformation, whose main energy source of the time would be Near-infrared laser irradiation, required the substances whose absorption is near the infrared, while the latter is the supreme focus of the current PTT research, which have been being developing for several decades. El-Sayed et al. showed the efficiency

of immunotargeted AuNPs as photothermal agents in living cells in vitro (44). The cancerous HOC and HSC cells suffer photothermal damage within 4 mins at laser energy thresholds (19 W/cm^2 and 25 W/cm^2), which are less than half that of healthy HaCaT cells (57 W/cm^2) (Fig. 3a).

Since the rise and ever-acceleration of PTT research, four generations of its nanomaterials have been developed, including noble-metal nanoparticles (45–52), graphitic nanostructures (53–55), colloidal nanocrystals consisted of metallic and non-metallic elements (56–59), and complex organic-dye compounds (60–67). Noble-metal nanoparticle represents the first-generation PTT nanomaterial attributed to their higher photothermal conversion efficiency, especially gold nanorods, yet this strategy costs too much, whereas their magnificent properties cannot be overlooked, still presenting a long-term cutting-edge investigation. Showing larger area of photothermal conversion but lower absorption capacity of NIR, graphitic nanostructures have become the second-generation materials of PTT; thereafter increasingly various materials and strategies have been considered for using as PTT agents. The third generation of PTT system comprising colloidal nanocrystals made of metallic and non-metallic elements is in the research craze recently, such as Cu/Se (56), Bi/S (57), Mo/Se (58), W/O (59), etc. As well, complex organic-dye compounds were reported its noticeably photothermal properties, becoming the fourth generation that has been being the latest research craze and keeping attracting attentions.

The mechanism of PTT has never been integrated consistently, instead varied research theory came up (68). El-Sayed et al. (69) used a real-time surface enhanced Raman spectroscopy to uncover the microcosmic process of hyperthermia-caused cell death. With laser irradiation, the protein tertiary structure was fading, by SRES analysis, because of the rupture of disulfide bonds, amide III, α-helix, β-sheet, etc. With exposure of laser, AuNPs was turning to local heat sources, caused destruction of proteins and lipids and then, finally, led to hyperthermia-induced cell death (Fig. 3b).

Apart from gold nanospheres applying for PTT, the most effective AuNPs using for PTT are gold nanorod (AuNR), contributed by their vast range of NIR windows. Decade ago, AuNR has been demonstrated as a specially promising candidate material for its tunable fabrication and fine LSPR property that AuNPs reveal a higher absorption cross-section at NIR frequencies. Huang et al. (70) designed an aptamer-based Au-AgNR (gold-silver nanorod), resulting a development in efficient and selective PTT for targeted tumor cell recognition; meanwhile, Au-AgNR required less energy than AuNRs. With aptamer labeled, 93% (±11) of cells have been induced to death by a relatively low power of laser irradiation and made decreasing side effect damage of surrounding tissues. Yi et al. (71) demonstrated an MMP-AuNR (matrix metalloprotease sensitive gold nanorod) in which MMP for bioimaging, both *in vivo* and *in vitro*, and AuNR for cancer PTT. Guo et al. (72) successfully fabricated a multifunctional nanocarriers based on CS-AuNR (chitosan/gold nanorod) by complexation and demonstrated this system could be used for bioimaging and PTT by *in vitro* experiments.

Further investigation has evaluated the photothermal therapeutic efficiency of various aspects of AuNRs. Mackey et al. (73) compared the photothermal therapeutic efficacy of three aspects of AuNRs theoretically and an *in vitro* experimentally. Summarizing consequences, the closer the maximum absorption peak is to the wavelength of the NIR laser irradiation, the better the hyperthermia effects.

To improving individual AuNR properties, Choi et al. (74) conjugated functional Pluronic nanocarriers on AuNR to stabilize AuNR as well as target drug delivery achieving combination PTT (Fig. 3c). Fen et al. (75) have replaced CTAB into poly(ethylene glycol) linked with 11-mercaptoundecanoic acid on AuNR surface, carrying Paclitaxel to present combination PTT. Presenting a similar but more succinct ligand, Liu et al. (76) grafted multidentate PEG to stabilize and biocompatibilize AuNR and then injected into tumor infected parts. With targeting NIR laser irradiation, the tumor cells have been proved wearing off. Chen et al. (77) reported a low-molecular-weight polyethylenimine-modified AuNR as a low cytotoxicity agent to treat tumor through photothermal route and diagnose with photoacoustic imaging, which can also transfect gene or drug efficiently. Sometimes with variety PTT materials involved together, the hyperthermia effect would be raised. Xu et al. (78) packaged AuNR in nanographene oxide, and, thus, these nanocomposites have increased both biocompatibility and hydrophilicity for better use in the biomedical field. Hyperthermia affects tumor tissues as well as brings collateral damages to normal tissues encompassed, and how to decrease the side effect is of the essence. Mooney et al. (79) reported a tumor-tropic therapeutic system based on PEG-grafted AuNRs and neural stem cells (NSC). PEG-grafted AuNRs were allowed to usher in the NSC to gain NSC-AuNR. Demonstrated NSC exhibited tumor-specific tropism, and NSC-AuNR showed the same property that it will close to tumor tissues meanwhile avoiding healthy tissues. Generally, collateral damages are come from the high intensity of laser, so mitigating the power of NIR laser is valuably investigable. Pan et al. (80) reported a nuclear location signal peptides-covered AuNR (AuNR-NLS), which only required low NIR irradiation of 0.2 W/cm^2 instead of normally above 0.4 W/cm^2 and even higher (75, 77, 81, 82), and the further *in vivo* experiments have indicated its biosafety and sufficiency.

Finding an appropriately reasonable carrier to conjugate AuNPs to achieve targeting delivery has been

always an attractive subject, and these kinds of carriers were reported variously. Liu et al. (83) creatively combined AuNR with silica dioxide shell and then grafted CXCR4 antibody, which was allowed to be recognized and introduced by pluripotent stem cells (iPS). Injecting these AuNRs-iPS systems into *in vivo* tumor lesion that exposed to NIR laser, the AuNRs would be released into tumor tissues, and hyperthermia would kill tumor cells, achieving PTT.

To make some significant progresses in stabilizing therapy agents, Li et al. (84, 85) coated natural mushroom β-glucans, a natural source product owning antitumor activity, over the AuNRs (AuNR-Glu) to somehow curtail its cytotoxicity and improve its colloidal stability; meanwhile, AuNR-Glu also presented anticancer activity and photothermal property.

Apart from AuNRs, there presents other simple morphological gold-based nanoparticles reported as photothermal therapeutic agents. Nam et al. (86) reported a brand-new proof-of-concept PTT based on plasmon modes of AuNPs, which shows aggregation in moderate acidic intracellular environment. The surface chemistry of this 'smart' AuNPs is designed to own both positive and negative charges by pH triggering that these AuNPs aggregated within acidic internal environment causing the red-shift to NIR for achieving PTT *in vivo*. Similar mechanism likewise, Gobin et al. (87) reported a series of NIR gold/silica nanoshells and gold/gold sulfide as an efficient PTT agent that would potentially ablate for tumor cells *in vitro* through hyperthermia induced by lasers irradiation. Wu et al. (88) explored the unusual optical property of gold nanocube (AuNC), compared with AuNR, that 45 nm AuNC demonstrated the high photoluminescence (PL) quantum yield and a remarkably enhanced extinction band at 544 nm, which would use for intracellular imaging and photothermal treatment, proving with intracellular experiments in human liver cancer cells (QGY) and human embryo kidney cells (293T). Aware nanoparticles whose absorption range is in NIR window will rise photothermal effects, even if a nanohybrid consisting of simply single no-NIR-absorption AuNPs could somehow reach the NIR window and demonstrated photothermal effects as well. Panikkanvalappil et al. (89) assembled dimer and pantamer Au nanoassemblies that can induce photothermal effects. With the development of gold nanoparticles, further more shaped AuNPs have been fabricated. Van de broke et al. (82) demonstrated a conjugation nanobody based on gold nanobranches whose lager absorption cross section is in NIR.

Developing with the further research, pure noble-metal nanoparticles have been grafted with some specific ligands for enhanced photothermal and targeted treatment effects. Wang et al. (90) have reported a sequence of supramolecularly assembled gold nanoparticles, which self-assembled β-CD-PEI (β-cyclodextrin grafted polyethylenimine), adamantine-PEG (Ad-PEG), and Ad-grafted 2 nm gold colloid into a gold supramolecular nanoparticle, in which Ad/β-CD played a role of recognition system. Then, its ligands were allowed to exchange into Ad-PEG(Arginylglycylaspartic acid) for recognizing certain tumor cell as a targeted treatment, and with optical irritation, it shows enhanced photothermal properties as well. Modifying for further applications, Jung et al. (91) have encompassed pH-responsive ligands on the surface of gold nanospheres as a 'turn-on' theragnostic agent for both simultaneously intracellular Raman imaging and PTT. Binding AuNPs with biomaterials, a new targeting therapeutic system was reported. Oh et al. (92) bond AuNPs on multi-peptide-grafted T7 phage that will both recognize prostate tumor cell and bind AuNPs to complete targeting PTT. Rengan et al. (93) utilized liposome as supporter frame to growth AuNPs, producing a AuNPs-coated liposome. After being injected in cell and irradiated by NIR laser, the LiposAuNPs have driven an increasing cell death rate. Sun et al. (94) conjugated a kind of thermally sensitive elastin-like polypeptides (ELP) to specific sites of AuNPs, producing a thermally sensitive ELP-AuNPs. Rising temperature led to an assembly of AuNPs that would present photothermal effects.

Multiple shapes of AuNPs can be used in multifunctional grafting as well, and Lu et al. (95) grafted prostate tumor cell recognition aptamers and antibodies on gold nanopopcorn for targeted therapy and photothermal response of prostate tumor cell SERS using irradiation, which occurred a brand-new strategy for targeted PTT. To strengthen photothermal effects, Bhana et al. (81) built gold nanopopcorn on the periphery of iron oxide cluster core, producing a magnetic-field-guided drug delivery system and combination treatment. Barbosa et al. (96) presented PEG-grafted gold nanostars and loading doxorubicin (DOX) chemically to target combined chemo-PTT. Pérez-Hernández et al. (97) utilized gold nanoprisms to present PTT research and exploited this to explore its molecular mechanism. Likewise, Tian et al. (98) grafted PEG and pH insertion peptides (pHLIPs) on gold nanostars orderly, gained good biocompatibility, and, with this agent, observed stronger signals in computed tomography (CT) and photoacoustic (PA) imaging. Be involved in some messy system, AuNPs could also present photothermal effects for combination therapeutic strategy. Wu et al. (99) reported a micelle as a cocktail therapeutic agent with photothermal effects and controlled drug release, which consists of lactose (LAC) and PEG-grafted polycysteine terpolymer (PC_{40}-*g*-PEG_5-LAC_5), 6-mercaptopurine (6-MP), doxorubicin (DOX), and AuNPs. Utilizing cross of materials to modified AuNPs acquiring promising therapy agents has presented these years. Xuan et al. (100) covered macrophage cell membrane on the surface of AuNPs-shelled porous silica

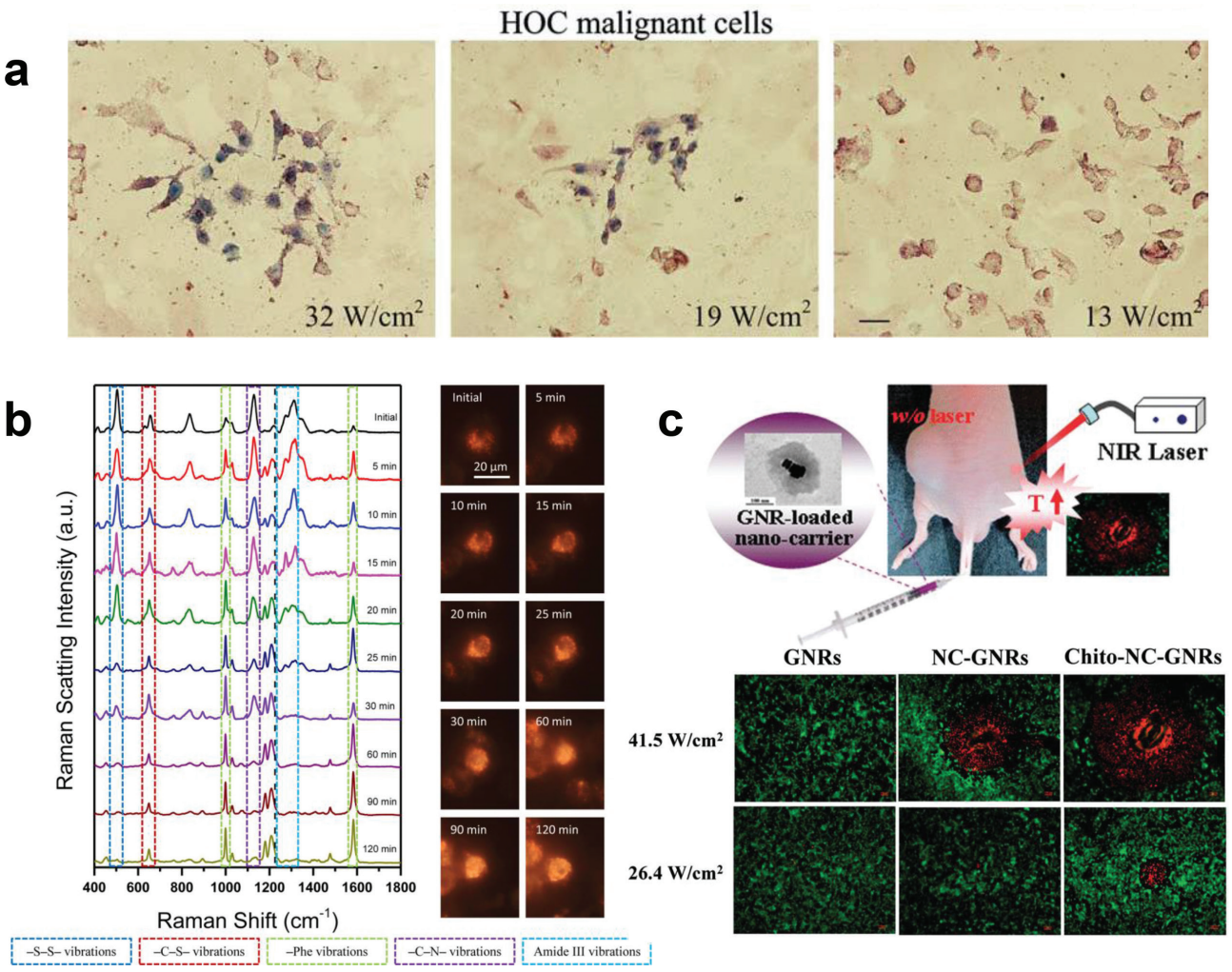

Fig. 3. (a) Oral squamous carcinoma cell lines (HOC malignant cells) loaded with AuNPs irradiated at different laser powers and were killed at and above 19 W/cm² (44). (b) Time-dependent surface-enhanced Raman scattering (SERS) spectra of single HSC-3 cell during PTT (69). (c) Fluorescence images after NIR PTT on SCC7 cancer cells (74).

nanoparticles to improve biocompatibility and load drugs simultaneously, presenting *in vivo* photothermal effects with NIR laser irradiation.

In most cases, the single therapy method often makes the therapeutic strategy demanding and unworkable. Developing multi-combination therapy is under the best importance. Combined chemo-PTT is investigated a lot, which somehow united therapeutic drugs and photothermal materials into one system, achieving more efficient therapy effects. Constant investigation has developed multi-combination methods and carriers. Loading drug by porous structure is a typical method for integration. An example described above (99) is beyond this way. As another detailed example, Yang et al. (101) reported that a triblock-engineered polypeptide $PC_{10}A(RGD)$ hydrogel-covered AuNR with the porous structure could intake DOX molecules, united therapeutic drugs, and photothermal materials subtly. With further decoration, targeting delivery and controllable release would be developed. Directly loading drug by chemical or physical interaction presented another way for integration. A previous example (96) is the use of this approach. The one more example is that Yi et al. (102) utilized DNA, which is grafted on AuNR, to accommodate DOX, and with laser stimulation to controlled release.

Conclusions and outlooks

Based on the broad range of plasmonic nanoparticles as basic building blocks, nanoassemblies with well-defined structure and functions can be designed for SERS-based biosensing and PTT theranostics. With the development of large-scale fabrication of nanoassemblies, it can be integrated with wearable electronics for real-time monitoring of human health. Also, more accurate nanostructures can be achieved by using both chemical modification and physical controlling. For example, direct observation of

the plasmon shift as a function of the coupling distance between nanoparticles has been exploited in several applications, such as the so-called plasmonic rulers, which are particularly useful for measuring biomolecular distances (103), detection of chemical moieties that may affect the size or conformation of the linker molecule, and for the generation of plasmonic barcodes by tuning the distance between two optically coupled silver disks (104, 105). In addition, close consideration of the energy distributions in the couplings among nanoassemblies suggests possible additional applications, such as photochemistry of molecules, metamaterial fabrication (106), optical switches (107), plasmonic waveguides, plasmon diodes, transmitting optical nanoantenna behavior (108), plasmon-assisted photothermal processes, or electrodes for single molecule conduction measurements (109). The plasmonic nanoassemblies can also be integrated with biodegradable polymers and loading drugs to achieve combined chemo-PTT to escalate therapeutic efficiency, which paves broad avenue for clinical theranostics and precise medicine.

Acknowledgments

This work was supported by the National Natural Science Foundation of China (21501027, 92163213, 11734005, 61821002, and 51628102), the National Key Research and Development Program of China (2021YFA1201403), the Applied Basic Research Program of Suzhou (SYG201911 and SYG201528), and the Fundamental Research Funds for the Central Universities (2242019k1G015). Y. Chen acknowledges the support from the Young Elite Scientists Sponsorship Program by China Association for Science and Technology (2015QNRC001), the Innovative and Entrepreneurial Talent Project of Jiangsu Province, and the Monash-JITRI Collaboration Fund. The authors also acknowledge the support from the Collaborative Innovation Center of Suzhou Nano Science and Technology.

Competing interest and funding

The authors declare that they have no known competing financial interests or personal relationships that could have appeared to influence the work reported in this paper.

Authors' contributions

Yi Chen: Conceptualization, Writing – original draft, Writing – review & editing, Visualization, Supervision, Project administration. Yu Bai: Writing – original draft, Writing – review & editing, Visualization. Heng Zhang: Writing – original draft, Writing – review & editing. Zheng Zhou: Writing – original draft, Writing – review & editing.

References

1. Alivisatos AP, Johnsson KP, Peng X, Wilson TE, Loweth CJ, Bruchez MP, Jr, et al. Organization of 'nanocrystal molecules' using DNA. Nature 1996; 382: 609–11. doi: 10.1038/382609a0
2. Maye MM, Kumara MT, Nykypanchuk D, Sherman WB, Gang O. Switching binary states of nanoparticle superlattices and dimer clusters by DNA strands. Nat Nanotechnol 2010; 5: 116–20. doi: 10.1038/nnano.2009.378
3. Nie Z, Fava D, Kumacheva E, Zou S, Walker GC, Rubinstein M. Self-assembly of metal-polymer analogues of amphiphilic triblock copolymers. Nat Matter 2007; 6(8): 609–14. doi: 10.1038/nmat1954
4. Liu K, Nie Z, Zhao N, Li W, Rubinstein M, Kumacheva E. Step-growth polymerization of inorganic nanoparticles. Science 2010; 329(5988): 197–200. doi: 10.1126/science.1189457
5. Pileni M-P. Self-assembly of inorganic nanocrystals: fabrication and collective intrinsic properties. Acc Chem Res 2007; 40(8): 685–93. doi: 10.1021/ar6000582
6. Heitsch AT, Patel RN, Goodfellow BW, Smilgies D-M, Korgel BA. GISAXS characterization of order in hexagonal monolayers of FePt nanocrystals. J Phys Chem C 2010; 114(34): 14427–32. doi: 10.1021/jp1047979
7. Jones MR, Macfarlane RJ, Lee B, Zhang J, Young KL, Senesi AJ, et al. DNA-nanoparticle superlattices formed from anisotropic building blocks. Nat Mater 2010; 9: 913–17. doi: 10.1038/nmat2870
8. Park SY, Lytton-Jean AKR, Lee B, Weigand S, Schatz GC, Mirkin CA. DNA-programmable nanoparticle crystallization. Nature 2008; 451: 553–6. doi: 10.1038/nature06508
9. Nykypanchuk D, Maye MM, van der Lelie D, Gang O. DNA-guided crystallization of colloidal nanoparticles. Nature 2008; 451: 549–52. doi: 10.1038/nature06560
10. Cheng WL, Hartman MR, Smilgies D-M, Long R, Campolongo MJ, Li R, et al. Probing in real time the soft crystallization of DNA-capped nanoparticles. Angew Chem Int Ed 2010; 49: 380–4. doi: 10.1002/anie.200904066
11. Schuller JA, Barnard ES, Cai W, Jun YC, White JS, Brongersma ML. Plasmonics for extreme light concentration and manipulation. Nat Matter 2010; 9(3): 193–204. doi: 10.1038/nmat2630
12. Shipway AN, Katz E, Willner I. Nanoparticle arrays on surfaces for electronic, optical, and sensor applications. ChemPhysChem 2000; 1(1): 18–52. doi: 10.1002/1439-7641(20000804)1:1%3C18::AID-CPHC18%3E3.0.CO;2-L
13. Ozbay E. Plasmonics: merging photonics and electronics at nanoscale dimensions. Science 2006; 311(5758): 189–93. doi: 10.1126/science.1114849
14. Anker JN, Hall WP, Lyandres O, Shah NC, Zhao J, Van Duyne RP. Biosensing with plasmonic nanosensors. Nat Matter 2008; 7(6): 442–53. doi: 10.1038/nmat2162
15. Maier SA, Kik PG, Atwater HA, Meltzer S, Harel E, Koel BE, et al. Local detection of electromagnetic energy transport below the diffraction limit in metal nanoparticle plasmon waveguides. Nat Matter 2003; 2(4): 229–32. doi: 10.1038/nmat852
16. Lal S, Clare SE, Halas NJ. Nanoshell-enabled photothermal cancer therapy: impending clinical impact. Acc Chem Res 2008; 41(12): 1842–51. doi: 10.1021/ar800150g
17. Yavuz MS, Cheng Y, Chen J, Cobley CM, Zhang Q, Rycenga M, et al. Gold nanocages covered by smart polymers for controlled release with near-infrared light. Nat Matter 2009; 8(12): 935–9. doi: 10.1038/nmat2564
18. Prodan E, Radloff C, Halas NJ, Nordlander P. A hybridization model for the plasmon response of complex nanostructures. Science 2003; 302(5644): 419–22. doi: 10.1126/science.1089171
19. Maye MM, Nykypanchuk D, Cuisinier M, van der Lelie D, Gang O. Stepwise surface encoding for high-throughput assembly of nanoclusters. Nat Mater 2009; 8(5): 388–91. doi: 10.1038/nmat2421

20. Lim D-K, Jeon K-S, Kim HM, Nam J-M, Suh YD. Nanogap-engineerable Raman-active nanodumbbells for single-molecule detection. Nat Mater 2010; 9(1): 60–7. doi: 10.1038/nmat2596
21. Xu X, Rosi NL, Wang Y, Huo F, Mirkin CA. Asymmetric functionalization of gold nanoparticles with oligonucleotides. J Am Chem Soc 2006; 128(29): 9286–7. doi: 10.1021/ja061980b
22. Zhang H, Wang R, Sikdar D, Wu L, Sun J, Gu N, et al. Plasmonic superlattice membranes based on bimetallic nanosea urchins as high-performance label-free surface-enhanced Raman spectroscopy platforms. ACS Sens 2022; 7(2): 622–31. doi: 10.1021/acssensors.1c02556
23. Chen Y, Yin H, Sikdar D, Yan L, Zhou Z, Sun J, et al. Gold nanopolyhedron-based superlattice sheets as flexible surface-enhanced Raman scattering sensors for detection of 4-aminothiophenol. ACS Appli Nano Mater 2021; 4(11): 12498–505. doi: 10.1021/acsanm.1c02884
24. Mulvaney P. Surface plasmon spectroscopy of nanosized metal particles. Langmuir 1996; 12(3): 788–800. doi: 10.1021/la9502711
25. Mie G. Beiträge zur Optik trüber Medien, speziell kolloidaler Metallösungen. Ann Phys 1908; 330(3): 377–445. doi: 10.1002/andp.19083300302
26. Liz-Marzán LM. Tailoring surface plasmons through the morphology and assembly of metal nanoparticles. Langmuir 2005; 22(1): 32–41. doi: 10.1021/la0513353
27. Kelly KL, Coronado E, Zhao LL, Schatz GC. The optical properties of metal nanoparticles: the influence of size, shape, and dielectric environment. J Phys Chem B 2002; 107(3): 668–77. doi: 10.1021/jp026731y
28. Tan SJ, Campolongo MJ, Luo D, Cheng WL. Building plasmonic nanostructures with DNA. Nat Nanotech 2011; 6: 268–76. doi: 10.1038/nnano.2011.49
29. Link S, El-Sayed MA. Size and temperature dependence of the plasmon absorption of colloidal gold nanoparticles. J Phys Chem B 1999; 103(21): 4212–17. doi: 10.1021/jp984796o
30. Rodriguez-Fernandez D, Langer J, Henriksen-Lacey M, Liz-Marzan LM. Hybrid Au–SiO2 core–satellite colloids as switchable SERS tags. Chem Mater 2015; 27(7): 2540–5. doi: 10.1021/acs.chemmater.5b00128
31. Rao VK, Radhakrishnan T. Tuning the SERS response with Ag-Au nanoparticle-embedded polymer thin film substrates. ACS Appl Mater Interf 2015; 7(23): 12767–73. doi: 10.1021/acsami.5b04180
32. Bai T, Sun J, Che R, Xu L, Yin C, Guo Z, et al. Controllable preparation of core–shell Au–Ag nanoshuttles with improved refractive index sensitivity and SERS activity. ACS Appl Mater Interf 2014; 6(5): 3331–40. doi: 10.1021/am405357v
33. Cui Q, Shen G, Yan X, Li L, Möhwald H, Bargheer M. Fabrication of Au@ Pt multibranched nanoparticles and their application to in situ SERS monitoring. ACS Appl Mater Interf 2014; 6(19): 17075–81. doi: 10.1021/am504709a
34. Shin H-S, Hong J-Y, Huh S. 2-Thiopheneacetic acid directed synthesis of Au nanorosette as an SERS-active substrate. ACS Appl Mater Interf 2013; 5(4): 1429–35. doi: 10.1021/am302865b
35. Xie W, Herrmann C, Kömpe K, Haase M, Schlücker S. Synthesis of bifunctional Au/Pt/Au core/shell nanoraspberries for in situ SERS monitoring of platinum-catalyzed reactions. J Am Chem Soc 2011; 133(48): 19302–5. doi: 10.1021/ja208298q
36. Sun Z, Du J, Yan L, Chen S, Yang Z, Jing C. Multifunctional Fe3O4@ SiO2–Au satellite structured SERS probe for charge selective detection of food dyes. ACS Appl Mater Interf 2016; 8(5): 3056–62. doi: 10.1021/acsami.5b10230
37. Sinha G, Depero LE, Alessandri I. Recyclable SERS substrates based on Au-coated ZnO nanorods. ACS Appl Mater Interf 2011; 3(7): 2557–63. doi: 10.1021/am200396n
38. Zhong L-B, Yin J, Zheng Y-M, Liu Q, Cheng X-X, Luo F-H. Self-assembly of Au nanoparticles on PMMA template as flexible, transparent, and highly active SERS substrates. Anal Chem 2014; 86(13): 6262–7. doi: 10.1021/ac404224f
39. Bekana D, Liu R, Amde M, Liu J-F. Use of polycrystalline ice for assembly of large area Au nanoparticle superstructures as SERS substrates. ACS Appl Mater Interf 2017; 9(1): 513–20. doi: 10.1021/acsami.6b15378
40. Zhao Y, Yang Y, Luo Y, Yang X, Li M, Song Q. Double detection of mycotoxins based on SERS labels embedded Ag@ Au core–shell nanoparticles. ACS Appl Mater Interf 2015; 7(39): 21780–6. doi: 10.1021/acsami.5b07804
41. MacLaughlin CM, Mullaithilaga N, Yang G, Ip SY, Wang C, Walker GC. Surface-enhanced Raman scattering dye-labeled Au nanoparticles for triplexed detection of leukemia and lymphoma cells and SERS flow cytometry. Langmuir 2013; 29(6): 1908–19. doi: 10.1021/la303931c
42. Jain PK, El-Sayed IH, El-Sayed MA. Au nanoparticles target cancer. Nano Today 2007; 2(1): 18–29. doi: 10.1016/S1748-0132(07)70016-6
43. Sokolov K, Follen M, Aaron J, Pavlova I, Malpica A, Lotan R, et al. Real-time vital optical imaging of precancer using anti-epidermal growth factor receptor antibodies conjugated to gold nanoparticles. Cancer Res 2003; 63(9): 1999–2004.
44. El-Sayed IH, Huang X, El-Sayed MA. Selective laser photo-thermal therapy of epithelial carcinoma using anti-EGFR antibody conjugated gold nanoparticles. Cancer Lett 2006; 239(1): 129–35. doi: 10.1016/j.canlet.2005.07.035
45. Huang X, El-Sayed IH, Qian W, El-Sayed MA. Cancer cell imaging and photothermal therapy in the near-infrared region by using gold nanorods. J Am Chem Soc 2006; 128(6): 2115–20. doi: 10.1021/ja057254a
46. Yamashita S, Fukushima H, Niidome Y, Mori T, Katayama Y, Niidome T. Controlled-release system mediated by a retro Diels-Alder reaction induced by the photothermal effect of gold nanorods. Langmuir 2011; 27(23): 14621–6. doi: 10.1021/la2036746
47. Khlebtsov BN, Panfilova EV, Terentyuk GS, Maksimova IL, Ivanov AV, Khlebtsov NG. Plasmonic nanopowders for photothermal therapy of tumors. Langmuir 2012; 28(24): 8994–9002. doi: 10.1021/la300022k
48. Wu P, Gao Y, Zhang H, Cai C. Aptamer-guided silver-gold bimetallic nanostructures with highly active surface-enhanced Raman scattering for specific detection and near-infrared photothermal therapy of human breast cancer cells. Anal Chem 2012; 84(18): 7692–9. doi: 10.1021/ac3015164
49. Bagley AF, Hill S, Rogers GS, Bhatia SN. Plasmonic photothermal heating of intraperitoneal tumors through the use of an implanted near-infrared source. ACS Nano 2013; 7(9): 8089–97. doi: 10.1021/nn4033757
50. Tsai M-F, Chang S-HG, Cheng F-Y, Shanmugam V, Cheng Y-S, Su C-H, et al. Au nanorod design as light-absorber in the first and second biological near-infrared windows for in vivo photothermal therapy. ACS Nano 2013; 7(6): 5330–42. doi: 10.1021/nn401187c
51. Abadeer NS, Murphy CJ. Recent progress in cancer thermal therapy using gold nanoparticles. J Phys Chem C 2016; 120(9): 4691–716. doi: 10.1021/acs.jpcc.5b11232
52. Ma N, Jiang YW, Zhang X, Wu H, Myers JN, Liu P, et al. Enhanced radiosensitization of gold nanospikes via hyperthermia in combined cancer radiation and photothermal therapy. ACS Appl Mater Interf 2016; 8(42): 28480–94. doi: 10.1021/acsami.6b10132

53. Yang K, Zhang S, Zhang G, Sun X, Lee ST, Liu Z. Graphene in mice: ultrahigh in vivo tumor uptake and efficient photothermal therapy. Nano Lett 2010; 10(9): 3318–23. doi: 10.1021/nl100996u
54. Su S, Wang J, Vargas E, Wei J, Martínez-Zaguilán R, Sennoune SR, et al. Porphyrin immobilized nanographene oxide for enhanced and targeted photothermal therapy of brain cancer. ACS Biomater Sci Eng 2016; 2(8): 1357–66. doi: 10.1021/acsbiomaterials.6b00290
55. Chen W, Zhang X, Ai F, Yang X, Zhu G, Wang F. Graphitic carbon nanocubes derived from ZIF-8 for photothermal therapy. Inorg Chem 2016; 55(12): 5750–2. doi: 10.1021/acs.inorgchem.6b01013
56. Hessel CM, Pattani VP, Rasch M, Panthani MG, Koo B, Tunnell JW, et al. Copper selenide nanocrystals for photothermal therapy. Nano Lett 2011; 11(6): 2560–6. doi: 10.1021/nl201400z
57. Liu J, Zheng X, Yan L, Zhou L, Tian G, Yin W, et al. Bismuth sulfide nanorods as a precision nanomedicine for in vivo multimodal imaging-guided photothermal therapy of tumor. ACS Nano 2015; 9(1): 696–707. doi: 10.1021/nn506137n
58. Lei Z, Zhu W, Xu S, Ding J, Wan J, Wu P. Hydrophilic MoSe2 nanosheets as effective photothermal therapy agents and their application in smart devices. ACS Appl Mater Interf 2016; 8(32): 20900–8. doi: 10.1021/acsami.6b07326
59. Zhao P, Ren S, Liu Y, Huang W, Zhang C, He J. PL-W18O49-TPZ nanoparticles for simultaneous hypoxia-activated chemotherapy and photothermal therapy. ACS Appl Mater Interf 2018; 10(4): 3405–13. doi: 10.1021/acsami.7b17323
60. Zheng M, Zhao P, Luo Z, Gong P, Zheng C, Zhang P, et al. Robust ICG theranostic nanoparticles for folate targeted cancer imaging and highly effective photothermal therapy. ACS Appl Mater Interf 2014; 6(9): 6709–16. doi: 10.1021/am5004393
61. Fu G, Liu W, Li Y, Jin Y, Jiang L, Liang X, et al. Magnetic Prussian blue nanoparticles for targeted photothermal therapy under magnetic resonance imaging guidance. Bioconjug Chem 2014; 25(9): 1655–63. doi: 10.1021/bc500279w
62. Zhang J, Liu S, Hu X, Xie Z, Jing X. Cyanine-curcumin assembling nanoparticles for near-infrared imaging and photothermal therapy. ACS Biomater Sci Eng 2016; 2: 1942–50. doi: 10.1021/acsbiomaterials.6b00315
63. Lin W, Li Y, Zhang W, Liu S, Xie Z, Jing X. Near-infrared polymeric nanoparticles with high content of cyanine for bimodal imaging and photothermal therapy. ACS Appl Mater Interf 2016; 8(37): 24426–32. doi: 10.1021/acsami.6b07103
64. Zhou B, Li Y, Niu G, Lan M, Jia Q, Liang Q. Near-infrared organic dye-based nanoagent for the photothermal therapy of cancer. ACS Appl Mater Interf 2016; 8(44): 29899–905. doi: 10.1021/acsami.6b07838
65. Wang S, Cao Y, Zhang Q, Peng H, Liang L, Li Q, et al. New application of old material: Chinese traditional ink for photothermal therapy of metastatic lymph nodes. ACS Omega 2017; 2(8): 5170–8. doi: 10.1021/acsomega.7b00993
66. Yoon HJ, Lee HS, Lim JY, Park JH. Liposomal indocyanine green for enhanced photothermal therapy. ACS Appl Mater Interf 2017; 9(7): 5683–91. doi: 10.1021/acsami.6b16801
67. Lin L, Liang X, Xu Y, Yang Y, Li X, Dai Z. Doxorubicin and indocyanine green loaded hybrid bicelles for fluorescence imaging guided synergetic chemo/photothermal therapy. Bioconjug Chem 2017; 28(9): 2410–19. doi: 10.1021/acs.bioconjchem.7b00407
68. Melamed JR, Edelstein RS, Day ES. Elucidating the fundamental mechanisms of cell death triggered by photothermal therapy. ACS Nano 2015; 9(1): 6–11. doi: 10.1021/acsnano.5b00021
69. Aioub M, El-Sayed MA. A real-time surface enhanced Raman spectroscopy study of plasmonic photothermal cell death using targeted gold nanoparticles. J Am Chem Soc 2016; 138(4): 1258–64. doi: 10.1021/jacs.5b10997
70. Huang Y-F, Sefah K, Bamrungsap S, Chang H-T, Tan W. Selective photothermal therapy for mixed cancer cells using aptamer-conjugated nanorods. Langmuir 2008; 24(20): 11860–5. doi: 10.1021/la801969c
71. Yi DK, Sun I-C, Ryu J-H, Koo H, Park CW, Youn I-C, et al. Matrix metalloproteinase sensitive gold nanorod for simultaneous bioimaging and photothermal therapy of cancer. Bioconjugate Chem 2010; 21(12): 2173–7. doi: 10.1021/bc100308p
72. Guo R, Zhang L, Qian H, Li R, Jiang X, Liu B. Multifunctional nanocarriers for cell imaging, drug delivery, and near-IR photothermal therapy. Langmuir 2010; 26(8): 5428–34. doi: 10.1021/la903893n
73. Mackey MA, Ali MR, Austin LA, Near RD, El-Sayed MA. The most effective gold nanorod size for plasmonic photothermal therapy: theory and in vitro experiments. J Phys Chem B 2014; 118(5): 1319–26. doi: 10.1021/jp409298f
74. Choi WI, Kim J-Y, Kang C, Byeon CC, Kim YH, Tae G. Tumor regression in vivo by photothermal therapy based on gold-nanorod-loaded, functional nanocarriers. ACS Nano 2011; 5(3): 1995–2003. doi: 10.1021/nn103047r
75. Ren F, Bhana S, Norman DD, Johnson J, Xu L, Baker DL, et al. Gold nanorods carrying paclitaxel for photothermal-chemotherapy of cancer. Bioconjug Chem 2013; 24(3): 376–86. doi: 10.1021/bc300442d
76. Liu X, Huang N, Li H, Wang H, Jin Q, Ji J. Multidentate polyethylene glycol modified gold nanorods for in vivo near-infrared photothermal cancer therapy. ACS Appl Mater Interf 2014; 6(8): 5657–68. doi: 10.1021/am5001823
77. Chen J, Liang H, Lin L, Guo Z, Sun P, Chen M, et al. Gold-nanorods-based gene carriers with the capability of photoacoustic imaging and photothermal therapy. ACS Appl Mater Interf 2016; 8(46): 31558–66. doi: 10.1021/acsami.6b10166
78. Xu C, Yang D, Mei L, Li Q, Zhu H, Wang T. Targeting chemo-photothermal therapy of hepatoma by gold nanorods/graphene oxide core/shell nanocomposites. ACS Appl Mater Interf 2013; 5(24): 12911–20. doi: 10.1021/am404714w
79. Mooney R, Roma L, Zhao D, Van Haute D, Garcia E, Kim SU, et al. Neural stem cell-mediated intratumoral delivery of gold nanorods improves photothermal therapy. ACS Nano 2014; 8(12): 12450–60. doi: 10.1021/nn505147w
80. Pan L, Liu J, Shi J. Nuclear-targeting gold nanorods for extremely low NIR activated photothermal therapy. ACS Appl Mater Interf 2017; 9(19): 15952–61. doi: 10.1021/acsami.7b03017
81. Bhana S, Lin G, Wang L, Starring H, Mishra SR, Liu G, et al. Near-infrared-absorbing gold nanopopcorns with iron oxide cluster core for magnetically amplified photothermal and photodynamic cancer therapy. ACS Appl Mater Interf 2015; 7(21): 11637–47. doi: 10.1021/acsami.5b02741
82. Van de Broek B, Devoogdt N, D'Hollander A, Gijs H-L, Jans K, Lagae L, et al. Specific cell targeting with nanobody conjugated branched gold nanoparticles for photothermal therapy. ACS Nano 2011; 5(6): 4319–28. doi: 10.1021/nn1023363
83. Liu Y, Yang M, Zhang J, Zhi X, Li C, Zhang C, et al. Human induced pluripotent stem cells for tumor targeted delivery of gold nanorods and enhanced photothermal therapy. ACS Nano 2016; 10(2): 2375–85. doi: 10.1021/acsnano.5b07172
84. Li X, Zhou J, Dong X, Cheng WY, Duan H, Cheung PCK. In vitro and in vivo photothermal cancer therapeutic effects of gold

nanorods modified with mushroom beta-glucan. J Agric Food Chem 2018; 66(16): 4091–8. doi: 10.1021/acs.jafc.8b00292
85. Li X, Zhou J, Liu C, Xiong Q, Duan H, Cheung PCK. Stable and biocompatible mushroom beta-Glucan modified gold nanorods for cancer photothermal therapy. J Agric Food Chem 2017; 65(43): 9529–36. doi: 10.1021/acs.jafc.7b03895
86. Nam J, Won N, Jin H, Chung H, Kim S. pH-Induced aggregation of gold nanoparticles for photothermal cancer therapy. J Am Chem Soc 2009; 131(38): 13639–45. doi: 10.1021/ja902062j
87. Gobin AM, Watkins EM, Quevedo E, Colvin VL, West JL. Near-infrared-resonant gold/gold sulfide nanoparticles as a photothermal cancer therapeutic agent. Small 2010; 6(6): 745–52. doi: 10.1002/smll.200901557
88. Wu X, Ming T, Wang X, Wang P, Wang J, Chen J. High-photoluminescence-yield gold nanocubes: for cell imaging and photothermal therapy. ACS Nano 2010; 4(1): 113–20. doi: 10.1021/nn901064m
89. Panikkanvalappil SR, Hooshmand N, El-Sayed MA. Intracellular assembly of nuclear-targeted gold nanosphere enables selective plasmonic photothermal therapy of cancer by shifting their absorption wavelength toward near-infrared region. Bioconjug Chem 2017; 28(9): 2452–60. doi: 10.1021/acs.bioconjchem.7b00427
90. Wang S, Chen KJ, Wu TH, Wang H, Lin WY, Ohashi M, et al. Photothermal effects of supramolecularly assembled gold nanoparticles for the targeted treatment of cancer cells. Angew Chem Int Ed Engl 2010; 49(22): 3777–81. doi: 10.1002/anie.201000062
91. Jung S, Nam J, Hwang S, Park J, Hur J, Im K, et al. Theragnostic pH-sensitive gold nanoparticles for the selective surface enhanced Raman scattering and photothermal cancer therapy. Anal Chem 2013; 85(16): 7674–81. doi: 10.1021/ac401390m
92. Oh MH, Yu JH, Kim I, Nam YS. Genetically programmed clusters of gold nanoparticles for cancer cell-targeted photothermal therapy. ACS Appl Mater Interf 2015; 7(40): 22578–86. doi: 10.1021/acsami.5b07029
93. Rengan AK, Bukhari AB, Pradhan A, Malhotra R, Banerjee R, Srivastava R, et al. In vivo analysis of biodegradable liposome gold nanoparticles as efficient agents for photothermal therapy of cancer. Nano Lett 2015; 15(2): 842–8. doi: 10.1021/nl5045378
94. Sun M, Peng D, Hao H, Hu J, Wang D, Wang K, et al. Thermally triggered in situ assembly of gold nanoparticles for cancer multimodal imaging and photothermal therapy. ACS Appl Mater Interf 2017; 9(12): 10453–60. doi: 10.1021/acsami.6b16408
95. Lu W, Singh AK, Khan SF, Senapati D, Yu H, Ray PC. Gold nano-popcorn-based targeted diagnosis, nanotherapy treatment, and in situ monitoring of photothermal therapy response of prostate cancer cells using surface-enhanced Raman spectroscopy. J Am Chem Soc 2010; 132(51): 18103–14. doi: 10.1021/ja104924b
96. Barbosa S, Topete A, Alatorre-Meda M, Villar-Alvarez EM, Pardo A, Alvarez-Lorenzo C, et al. Targeted combinatorial therapy using gold nanostars as theranostic platforms. J Phys Chem C 2014; 118(45): 26313–23. doi: 10.1021/jp505979e
97. Pérez-Hernández M, del Pino P, Mitchell SG, Moros M, Stepien G, Pelaz B, et al. Dissecting the molecular mechanism of apoptosis during photothermal therapy using gold nanoprisms. ACS Nano 2015; 9(1): 52–61. doi: 10.1021/nn505468v
98. Tian Y, Zhang Y, Teng Z, Tian W, Luo S, Kong X, et al. pH-Dependent transmembrane activity of peptide-functionalized gold nanostars for computed tomography/photoacoustic imaging and photothermal therapy. ACS Appl Mater Interf 2017; 9(3): 2114–22. doi: 10.1021/acsami.6b13237
99. Wu X, Zhou L, Su Y, Dong CM. Plasmonic, targeted, and dual drugs-loaded polypeptide composite nanoparticles for synergistic cocktail chemotherapy with photothermal therapy. Biomacromolecules 2016; 17(7): 2489–501. doi: 10.1021/acs.biomac.6b00721
100. Xuan M, Shao J, Dai L, Li J, He Q. Macrophage cell membrane camouflaged Au nanoshells for in vivo prolonged circulation life and enhanced cancer photothermal therapy. ACS Appl Mater Interf 2016; 8(15): 9610–18. doi: 10.1021/acsami.6b00853
101. Yang J, Yao M-H, Jin R-M, Zhao D-H, Zhao Y-D, Liu B. Polypeptide-engineered hydrogel coated gold nanorods for targeted drug delivery and chemo-photothermal therapy. ACS Biomater Sci Eng 2017; 3(10): 2391–8. doi: 10.1021/acsbiomaterials.7b00359
102. Yi Y, Wang H, Wang X, Liu Q, Ye M, Tan W. A smart, photocontrollable drug release nanosystem for multifunctional synergistic cancer therapy. ACS Appl Mater Interf 2017; 9(7): 5847–54. doi: 10.1021/acsami.6b15414
103. Reinhard BM, Sheikholeslami S, Mastroianni A, Alivisatos AP, Liphardt J. Use of plasmon coupling to reveal the dynamics of DNA bending and cleavage by single EcoRV restriction enzymes. Proc Natl Acad Sci U S A 2007; 104(8): 2667–72. doi: 10.1073/pnas.0607826104
104. Romo-Herrera JM, Alvarez-Puebla RA, Liz-Marzan LM. Controlled assembly of plasmonic colloidal nanoparticle clusters. Nanoscale 2011; 3(4): 1304–15. doi: 10.1039/c0nr00804d
105. Banholzer MJ, Osberg KD, Li S, Mangelson BF, Schatz GC, Mirkin CA. Silver-based nanodisk codes. ACS Nano 2010; 4(9): 5446–52. doi: 10.1021/nn101231u
106. Smith DR, Pendry JB, Wiltshire MCK. Metamaterials and negative refractive index. Science 2004; 305(5685): 788–92. doi: 10.1126/science.1096796
107. Large N, Abb M, Aizpurua J, Muskens OL. Photoconductively loaded plasmonic nanoantenna as building block for ultracompact optical switches. Nano Lett 2010; 10(5): 1741–6. doi: 10.1021/nl1001636
108. Aeschlimann M, Bauer M, Bayer D, Brixner T, Garcia de Abajo FJ, Pfeiffer W, et al. Adaptive subwavelength control of nano-optical fields. Nature 2007; 446(7133): 301–4. doi: 10.1038/nature05595
109. Dadosh T, Gordin Y, Krahne R, Khivrich I, Mahalu D, Frydman V, et al. Measurement of the conductance of single conjugated molecules. Nature 2005; 436(7051): 677–80. doi: 10.1038/nature03898

***Yi Chen**
Email: yichen@seu.edu.cn